# Lattice dynamical effects on the Peierls transition in one-dimensional metals and spin chains

Holger Fehske, Michael Holicki, Alexander Weiße

Physikalisches Institut, Universität Bayreuth, D-95440 Bayreuth

**Summary:** The interplay of charge, spin and lattice degrees of freedom is studied for quasi-one-dimensional electron and spin systems coupled to quantum phonons. Special emphasis is put on the influence of the lattice dynamics on the Peierls transition. Using exact diagonalization techniques the ground-state and spectral properties of the Holstein model of spinless fermions and of a frustrated Heisenberg model with magneto-elastic coupling are analyzed on finite chains. In the non-adiabatic regime a ($T = 0$) quantum phase transition from a gapless Luttinger-liquid/spin-fluid state to a gapped dimerized phase occurs at a nonzero critical value of the electron/spin-phonon interaction. To study the nature of the spin-Peierls transition at finite temperatures for the infinite system, an alternative Green's function approach is applied to the magnetostrictive XY model. With increasing phonon frequency the structure factor shows a remarkable crossover from soft-mode to central-peak behaviour. The results are discussed in relation to recent experiments on $CuGeO_3$.

## 1 Introduction

Low dimensional electronic materials are known to be very susceptible to structural distortions driven by the electron-phonon interaction. Probably the most famous one is the Peierls instability [1] of one-dimensional (1D) metals: as the temperature is lowered the system creates a periodic variation in charge density, called a "charge-density-wave" (CDW), by shifting the electrons and ions from their symmetric positions. For the half-filled band case the CDW is commensurate with the lattice and cannot slide as a whole. As a result the unit cell is doubled and the system has a broken-symmetry ground state. Since the dimerization of the lattice opens a gap at the Fermi surface the Peierls process transforms a metal into an insulator. Spontaneous dimerization transitions to a less symmetric but lower-energy configuration like those shown in Fig. 1 (left panel) have been found in many quasi-1D materials, such as the organic conjugated polymers [e.g., $(CH)_x$] and charge transfer salts [e.g., TTF(TCNQ)] or the inorganic blue bronzes [e.g., $K_{0.3}MoO_3$] and MX-chains [2].

As a generic theoretical model for such systems the 1D Hubbard model is frequently considered,

$$\mathcal{H}_{\rm e} = -\sum_{i,\sigma} t_{ii} n_{i\sigma} - \sum_{i,\sigma} t_{ii+1} (c_{i\sigma}^{\dagger} c_{i+1\sigma} + \text{H.c.}) + U \sum_{i} n_{i\uparrow} n_{i\downarrow}\,, \tag{1.1}$$

supplemented by a coupling to the phonon system

$$\mathcal{H}_{\rm p} = \sum_{i} \frac{p_i^2}{2M} + \frac{K}{2} q_i^2 \tag{1.2}$$

according to

$$\begin{array}{rccc} \text{SSH-type [3]:} & t_{ii} = 0 & t_{ii+1} \to t(1+\lambda q_i) & q_i = u_i - u_{i+1} \\ \text{Holstein-type [4]:} & t_{ii} \to \lambda q_i & t_{ii+1} = t & q_i = u_i\,, \end{array} \tag{1.3}$$

i.e., the lattice vibrations $q_i$ interact with the electrons by modifying the electron hopping matrix element $t_{ij}$ and on–site potential $t_{ii}$, respectively. In Eq. (1.1), $c_{i\sigma}^{\dagger}$ ($c_{i\sigma}$) creates (annihilates) a spin-$\sigma$ electron at Wannier site $i$, and $n_{i\sigma} = c_{i\sigma}^{\dagger} c_{i\sigma}$.

If there is one electron per site and the Coulomb repulsion is strong, $U \gg t$, we are in the limit of localized electrons interacting via an effective antiferromagnetic (AF) exchange interaction $J$ ($\propto t^2/U$) and the system can be described by an Heisenberg Hamiltonian with magneto-elastic coupling [5]

$$\mathcal{H} = -J \sum_{i} (1 + \lambda q_i) \vec{S}_i \vec{S}_{i+1} + \mathcal{H}_{\rm p}\,, \tag{1.4}$$

where $\vec{S}_i = \sum_{\sigma\sigma'} \tilde{c}_{i\sigma}^{\dagger} \vec{\tau}_{\sigma\sigma'} \tilde{c}_{i\sigma'}$ with $\tilde{c}_{i\sigma}^{(\dagger)} = c_{i\sigma}^{(\dagger)} (1 - \tilde{n}_{i,-\sigma})$. In analogy to the Peierls instability in 1D metals, the dependence of $J$ on the distance between neighbouring spins again gives rise to an instability, where the energy of the spin chain is lowered by dimerizing into an alternating pattern of weak and strong bonds. This so-called "spin-Peierls" (SP) transition leads to the formation of a singlet (dimer) ground state and there is an energy gap to elementary (massive) spin triplet excitations being well-separated from the continuum [see Fig. 1 (right panel)]. Experimentally, the SP phenomenon was observed in a number of organic compounds, such as (TTF)(CuBDT) or MEM$(\text{TCNQ})_2$ [6].

Most theoretical treatments of the Peierls instability describe the lattice degrees of freedom classically. In a wide range quasi-1D metals, however, the lattice zero-point motion is comparable to the Peierls lattice distortion, which makes the rigid lattice approximation questionable [7]. By any means lattice dynamical (quantum phonon) effects should be included in a theoretical analysis of the extraordinary transport and optical phenomena observed in Peierls-distorted systems [8, 9]. Likewise the interest in models of spins coupled dynamically to phonons has increased significantly since it was recognized that the first inorganic

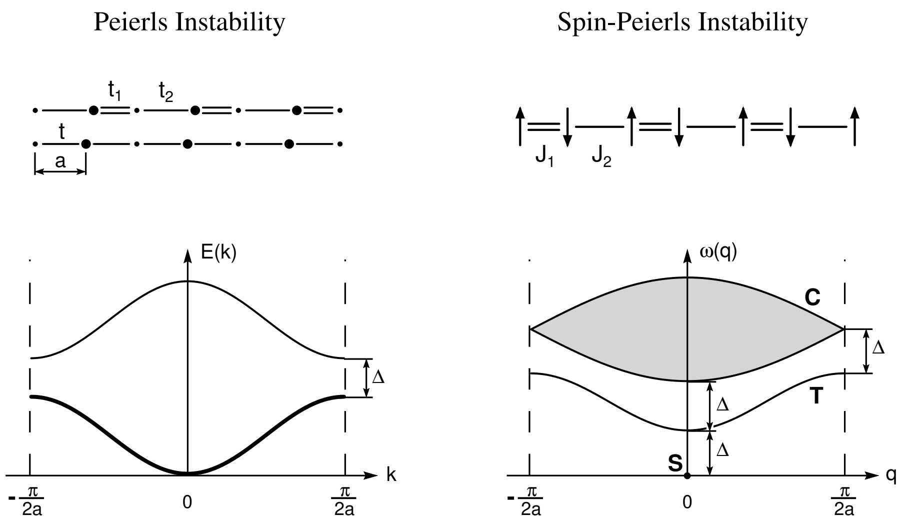


**Figure 1** Schematic representation of the Peierls- and spin-Peierls scenarios. The left panel shows the opening of a gap $\Delta$ in the electronic band structure $E(k)$ of an 1D metal at the Fermi surface if, according to an SSH- or Holstein-type of electron-phonon coupling, a static lattice distortion with the new lattice period $2a$ occurs. The right panel represents the main features of the excitation spectrum of a Peierls-distorted 1D quantum spin chain. Above the singlet (S) ground state at least one elementary excitation, corresponding e.g. to a triplet (T) bound state, is split from the continuum (C).

SP compound $CuGeO_3$ [10] shows no clear separation between the magnetic and phononic energy scales: the two (weakly dispersive optical) Peierls-active $T_2^+$ phonon modes have frequencies $\omega_{0,1} \simeq J$ and $\omega_{0,2} \simeq 2J$ [11, 12]. Moreover, in contrast to the organic SP materials, no phonon-softening is observed at the SP transition [13]. The SP physics in $CuGeO_3$ is therefore in the non-adiabatic regime.

Motivated by this situation, in this report, we study the perhaps minimal microscopic models capable of describing the Peierls and spin-Peierls transitions in 1D systems by the use of numerical techniques allowing an essentially exact treatment of both subsystems, electrons/spins and phonons, at a fully quantum-mechanically level. In the weak-coupling regime, the random-phase-approximation (RPA) approach is shown to be consistent not only with phonon softening but also with phonon hardening at the SP transition, as observed, e.g., in (TTF)(CuBDT) and $CuGeO_3$, respectively.

## 2 Luttinger-liquid vs. charge-density-wave behaviour

First we consider the 1D Hubbard model, Eq. (1.1), at quarter filling and confine ourselves to the case of spinless fermions for simplicity. This model is of physical relevance in the strong interaction limit $U \to \infty$ and is particularly interesting because a quantum phase transition from a Luttinger liquid (LL) to a CDW phase occurs at a finite electron-phonon interaction, demonstrating that the quantum phonon fluctuations destroy the dimerized ground state for weak electron-phonon couplings [14, 15].

Rescaling $\mathcal{H} \to \mathcal{H}/t = \bar{\mathcal{H}}_{\mathrm{e}} + \bar{\mathcal{H}}_{\mathrm{p}} + \bar{\mathcal{H}}_{\mathrm{ep}}$ and setting

$$\lambda = g\sqrt{2K\omega_0} \qquad \text{with} \qquad \omega_0^2 = K/M \tag{2.5}$$

the Holstein Hamiltonian in a particle-hole symmetric notation is given by

$$\bar{\mathcal{H}}_{\mathrm{e}} = -\sum_i (c_i^\dagger c_{i+1} + c_{i+1}^\dagger c_i)\ , \quad \bar{\mathcal{H}}_{\mathrm{p}} = \omega_0 \sum_i (b_i^\dagger b_i + \tfrac{1}{2})\ , \tag{2.6}$$

and

$$\bar{\mathcal{H}}_{\mathrm{e-p}} = -g\omega_0 \sum_i (b_i^\dagger + b_i)\,(n_i - \tfrac{1}{2})\ . \tag{2.7}$$

In Eqs. (2.6) and (2.7), $b_i^{(\dagger)}$ annihilates (creates) a dispersionsless Einstein phonon of frequency $\omega_0$ coupled to the local electron density $n_i = c_i^\dagger c_i$ ($\hbar = 1$, and all energies are measured in units of $t$). Note that for the Holstein model the dimensionless electron-phonon coupling constant $g = \sqrt{\varepsilon_p/\omega_0}$ is directly related to the familiar polaron shift $\varepsilon_p$ being a second natural measure of the strengths of the electron-phonon interaction. Both parameters are necessary in order to characterize the weak ($\varepsilon_p \ll 1$) and strong coupling ($\varepsilon_p \gg 1$ *and* $g \gg 1$) situations in the adiabatic ($\omega_0 \ll 1$) and anti-adiabatic regimes ($\omega_0 \gg 1$), respectively.

Previous results for the ground-state phase diagram of the Holstein model at half-filling obtained by WL QMC [14] and GF MC [16] simulations showed significant discrepancies in the region of small $\omega_0$ ($0 < \omega_0 \lesssim 1$). Only very recently Bursill et al. [15] provided more reliable information from level crossings in their DMRG data. Applying a new optimized phonon approach for the diagonalization of coupled electron/spin-phonon systems [17], we consider the Holstein model on chains of even length with up to 10 sites and periodic (antiperiodic) boundary conditions if there is an odd (even) number of fermions in the system. The resulting phase diagram is shown in Fig. 2 over a wide range of frequencies and coupling strengths. For small $g$ the system is a metal, more precisely a Luttinger liquid with parameters that vary with the coupling (see below). For large $g$ the system has an energy gap and develops true long-range CDW order in the thermodynamic limit. The phase boundary obtained with our optimized

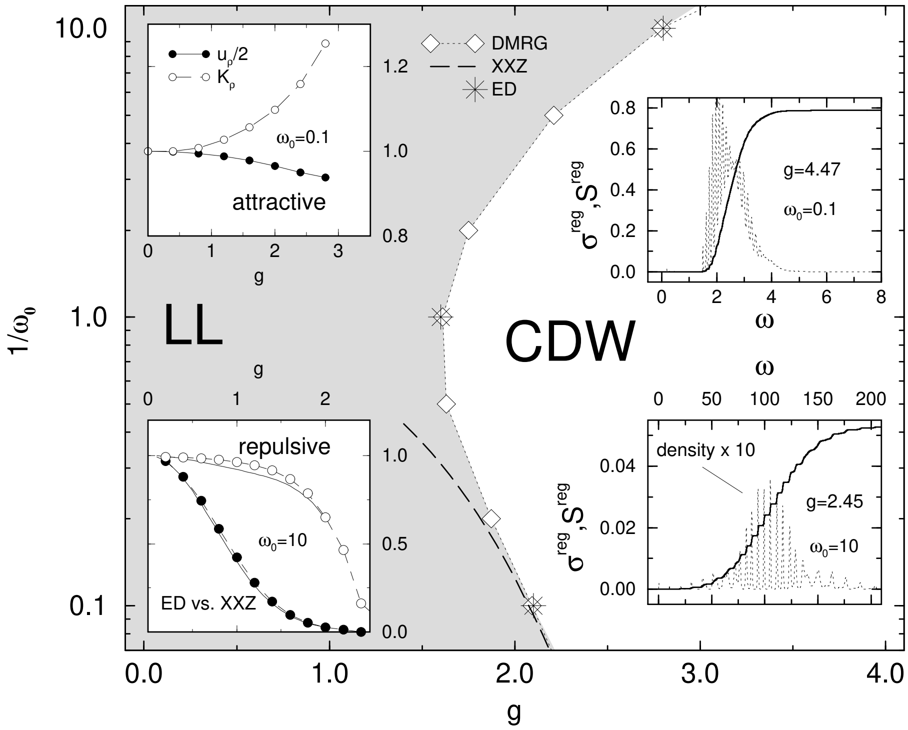


**Figure 2** Ground-state phase diagram of the 1D Holstein model of spinless fermions at half-filling ($N_e = N/2$), showing the boundary between the Luttinger liquid (LL) and charge-density-wave (CDW) states obtained by exact diagonalization (ED) and density matrix renormalization group (DMRG) [15] approaches. The dashed line gives the asymptotic result for the XXZ model. Left insets show the LL parameters $u_\rho$ and $K_\rho$ as a function of the electron-phonon $g$ in the metallic regime; right insets display for a six-site chain the regular part of the optical conductivity $\sigma^{reg}(\omega)$ (dotted lines) and the integrated spectral weight $\mathcal{S}^{reg}(\omega) = \int_0^\omega d\omega' \sigma^{reg}(\omega')$ (solid lines) in the CDW region.

phonon diagonalization methods agrees with recent DMRG results [15]. In the adiabatic limit $\omega_0 = 0$, the critical coupling converges to zero, as expected for the Holstein Hamiltonian, Eqs. (1.1)-(1.3), with $M \to \infty$. For $0 < \omega_0 \lesssim 1$ the accurate determination of $g_c$ is somewhat difficult. On the other hand, in the strong-coupling anti-adiabatic regime, the half-filled Holstein model can be transformed to the exactly soluble XXZ (small polaron) model [14, 18]

$$\bar{\mathcal{H}}^{\mathrm{XXZ}} = \frac{N}{4}(2\omega_0 - g^2\omega_0 - V_2) - \mathrm{e}^{-g^2} \sum_i \left[ (S_i^+ S_{i+1}^- + S_i^- S_{i+1}^+) - V_2\, \mathrm{e}^{g^2} S_i^z S_{i+1}^z \right] \tag{2.8}$$

using second order perturbation theory with respect to $t$. Here $V_2(g^2,\omega_0) = 2e^{-2g^2}\omega_0^{-1}\sum_{s\neq 0}(2g^2)^s/(ss!)$, and the (Kosterlitz-Thouless) phase transition line is given by the condition $V_2(\alpha,g^2)\mathrm{e}^{g^2}/2 = 1$ (long-dashed curve in Fig. 2).

Let us now characterize the LL and CDW phases in some more detail. According to Haldane's Luttinger liquid conjecture [19], 1D gapless systems of interacting fermions should belong to the same universality class as the Tomonaga-Luttinger model. As stated above, the Holstein system is gapless for small enough coupling $g$. Thus it is obvious to prove, following the lines of approach to the problem by McKenzie et al. [16], whether our Lanczos data shows a finite-size scaling like a Luttinger liquid. For a LL of spinless fermions, the ground-state energy $E_0(N)$ of a finite system of $N$ sites scales to leading order as

$$\frac{E_0(N)}{N} = \epsilon_\infty - \frac{\pi u_\rho}{6N^2}\,, \tag{2.9}$$

where $\epsilon_\infty$ denotes the ground-state energy per site for the infinite system and $u_\rho$ is the velocity of the charge excitations. If $E_{\pm 1}(N)$ is the ground-state energy with $\pm 1$ fermions away from half filling, to leading order the scaling should be

$$E_{\pm 1}(N) - E_0(N) = \frac{\pi u_\rho}{2K_\rho N}\,. \tag{2.10}$$

$K_\rho$ is the renormalized effective coupling (stiffness) constant. The left insets of Fig. 2 show the LL parameters as a function of $g$ in the region, where the scaling relations Eqs. (2.9) and (2.10) hold. A very interesting result is the changing character of the interaction below $\omega_0 \sim 1$. For small frequencies the effective fermion-fermion interaction is attractive, while it is repulsive for large frequencies, where the system forms a polaronic metal with strongly reduced kinetic energy [17]. Self-evidently there is a transition line in between, where the model describes "free" particles in lowest order.

In the CDW state extremely valuable information about the low-energy excitations can be obtained from the behaviour of the optical conductivity. The real part of $\sigma(\omega)$ contains two contributions, the (coherent) Drude part at $\omega = 0$ and a so-called "regular term", $\sigma^{reg}(\omega)$, due to finite-frequency dissipative optical transitions to excited quasiparticle states. In spectral representation ($T = 0$), the regular part takes the form

$$\sigma^{reg}(\omega) = \sum_{m>0} \frac{|\langle\Psi_0|i\sum_j(c_j^\dagger c_{j+1} - c_{j+1}^\dagger c_j)|\Psi_m\rangle|^2}{E_m - E_0}\,\delta[\omega - (E_m - E_0)]\,, \tag{2.11}$$

where $\sigma^{reg}(\omega)$ is given in units of $\pi e^2$ and we have omitted an $1/N$ prefactor. The evaluation of dynamical correlation functions, such as Eq. (2.11), can be carried out by means of very efficient and numerically stable Chebyshev recursion and maximum entropy algorithms [20]. Clearly the optical absorption spectrum in the strong EP coupling regime is quite different from that in the LL phase (cf. Ref. [21]). It can be interpreted in terms of strong electron-phonon correlations and corroborates the CDW picture. Since for $g > g_c$ the electronic band structure is gapped we expect that the low-energy gap feature survives in the thermodynamic limit. In the adiabatic region (upper right inset), the broad optical absorption band is produced by a single-particle excitation accompanied by multi-phonon absorptions and is basically related to the lowest unoccupied state of the upper band of the CDW insulator. The lineshape of $\sigma^{reg}(\omega)$ reflects the phonon distribution in the ground state. The most striking feature is the large spectral weight contained in the incoherent part of optical conductivity. Moreover, employing the f-sum rule for the optical conductivity [22] and taking into account the behaviour of the kinetic energy ($\propto u_\rho$) as function of $g$, we found that in the metallic LL and insulating CDW phases nearly all the spectral weight is contained in the coherent (Drude) and incoherent (regular) part of Re $\sigma(\omega)$, respectively. As stated above, in the anti-adiabatic regime the LL phase is basically a polaronic metal, i.e., the electrons will be heavily dressed by phonons. Since the renormalized coherent bandwidth of the polaron band is extremely small, the finite-size gaps in the band structure are reduced as well. Therefore, the gap occurring in the CDW state ($\Delta_{CDW} \sim \varepsilon_p$) may be identified with the optical absorption threshold (see lower right inset).

## 3 Non-adiabatic approach to the spin-Peierls transition

### 3.1 Exact diagonalization results for T=0

In spite of the experimental fact that a realistic modeling of the inorganic SP compound $CuGeO_3$ should include the phonon dynamics, previous theoretical studies have commonly adopted an alternating and frustrated AF Heisenberg spin chain model [23]

$$\bar{\mathcal{H}}^{\text{static}} = \sum_i \Big[(1+\delta(-1)^i)\vec{S}_i\vec{S}_{i+1} + \alpha\,\vec{S}_i\vec{S}_{i+2}\Big] \tag{3.12}$$

with a static dimerization parameter $\delta$, thus representing the extreme adiabatic limit of a SP chain (in this section all energies are given in units of $J$). $\alpha$ determines the strength of the frustrating AF next-nearest-neighbour coupling. The spin model (3.12) contains two independent mechanisms for spin gap formation. At $\delta = 0$ and for $\alpha < \alpha_c$ the ground state is a spin liquid and the elementary excitations are massless spinons [24]. The critical value of frustration $\alpha_c = 0.241$ was accurately determined by numerical studies [23, 25]. For $\alpha > \alpha_c$ the ground state is spontaneously dimerized, the spectrum acquires a gap, and the elementary excitations are massive spinons [26, 27]. On the other hand for any finite $\delta$, the singlet ground state of the model (3.12) is also dimerized, but the elementary excitation is a massive magnon [24, 28]. A comprehensive study of the spectral properties of the model (3.12) in terms of the spin dynamical structure factor has been carried out by Yokoyama and Saiga [29].

From the magnetic properties of the uniform phase $J \simeq 160$ K and $\alpha = 0.36$ have been estimated for $CuGeO_3$ [30]. However, if one attempts to reproduce the observed spin gap $\Delta^{\mathrm{ST}} \simeq 2.1$ meV within the static model (3.12), a very small value of $\delta \simeq 1.2\%$ results. From the uniaxial pressure derivatives of the exchange coupling $J$ [31] and the structural distortion in the dimerized phase [11] a minimum magnetic dimerization of about 4% is obtained, incompatible with an adiabatic approach to the SP transition.

The simplest model that maintains the full quantum dynamics of the lattice vibrations may be obtained from Eq. (3.12) by replacing $(-1)^i\delta \to g\omega_0(b_i^\dagger + b_i)$:

$$\bar{\mathcal{H}}_{\mathrm{s}} = \sum_i (\vec{S}_i\vec{S}_{i+1} + \alpha\vec{S}_i\vec{S}_{i+2}) \,, \quad \bar{\mathcal{H}}_{\mathrm{p}} = \omega_0 \sum_i b_i^\dagger b_i \,, \tag{3.13}$$

$$\bar{\mathcal{H}}_{\mathrm{sp}}^{\mathrm{I}} = g\omega_0 \sum_i (b_i^\dagger + b_i)\vec{S}_i\vec{S}_{i+1} \,. \tag{3.14}$$

Recently it was shown that such a dynamical spin-phonon model describes the general features of the magnetic excitation spectrum of $CuGeO_3$ [32, 33, 34]. Here we focus on the behaviour of the lattice dimerization which can be found from the displacement structure factor at wave number $q = \pi$

$$\delta^2 = \left(\frac{g\omega_0}{N}\right)^2 \sum_{i,j} C_{ij}^{uu} \mathrm{e}^{\mathrm{i}\pi(R_i - R_j)} \quad \text{with} \quad C_{ij}^{uu} = \langle (b_i + b_i^\dagger)(b_j + b_j^\dagger) \rangle \,. \tag{3.15}$$

The alternating structure of the correlation function $C_{1i}$ as shown in the inset Fig. 3 (a) implies the Peierls formation of short and long bonds and thus alternating strong and weak AF exchange interactions, i.e., a dimerized ground state. The structure is enhanced (weakened) increasing the spin–phonon coupling (phonon frequency) [32]. As in the ordinary Peierls phenomenon, a finite dimerization $\delta > 0$ necessarily leads to a gap $\Delta^{\mathrm{ST}}$ in the magnetic excitation spectrum. For evaluating the relation between the dimerization and the resulting magnitude of the spin triplet excitation gap, we keep the phonon frequency fixed, vary the coupling strength $g$ and calculate for each parameter set $\Delta^{\mathrm{ST}} = E_0^{\mathrm{T}} - E_0^{\mathrm{S}}$ and the dimerization $\delta$ from Eq. (3.15). ED results for $\Delta^{\mathrm{ST}}$ obtained for the static spin-only model (3.13) and the quantum phonon model (3.14) are compared in the main part of Fig. 3 (a). For vanishing dimerization, i.e. in the absence of any spin–phonon coupling ($g = 0$) the results for the static and the dynamic model naturally agree (note that for $\delta = 0$ there remains a spin excitation gap due to the frustration driven singlet dimer ordering). The dynamic model (3.14) partially resolves the $\Delta^{\mathrm{ST}} - \delta$ conflict we are faced within the static approach,

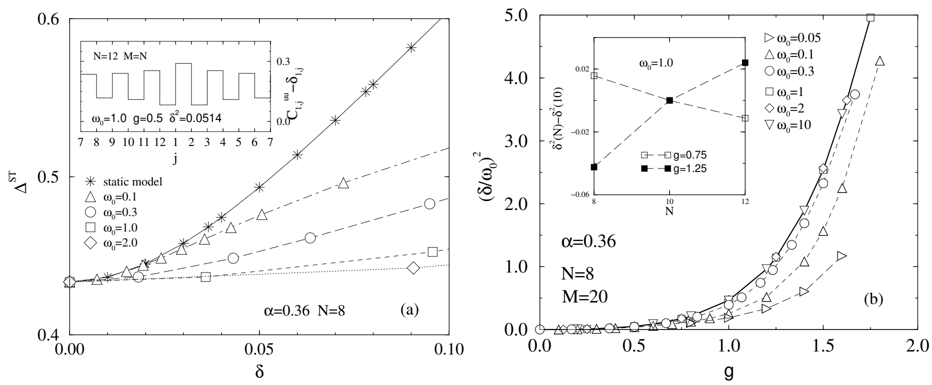


**Figure 3** Spin gap (a) and dimerization (b) in the frustrated Heisenberg spin chain with dynamical spin-phonon coupling.

because the dimerization $\delta$ grows with the phonon frequency at fixed $\Delta^{\mathrm{ST}}$. Thus matching $\Delta^{\mathrm{ST}}$ to the neutron scattering data, a larger $\delta \simeq 5\%$ may result.

Figure 3 (b) shows the dimerization as a function of the spin-phonon interaction strength. As for the Holstein model the precise determination of the critical coupling $g_c$ is difficult for phonons in the adiabatic regime $\omega_0 < 0.5$. On the contrary, in the non-adiabatic regime the SP transition takes place at $g_c \simeq 1$ nearly irrespective of $\omega_0$. Most remarkably, below (above) $g_c$ the dimerization decreases (increases) with increasing lattice size $N$ (see inset), indicating that the infinite system exhibits a true phase transition.

### 3.2 Anti-adiabatic limit: mapping to an effective magnetic problem

Figure 3 (b) implies that more insight into the dynamic spin-phonon model can be obtained by considering the limit of large phonon frequencies. One can then integrate out the lattice degrees of freedom in order to derive an effective spin Hamiltonian which cover the dynamical effect of phonons in a approximate way. Technically this can be achieved by a variety of methods, such as standard perturbation theory [35], continuous (flow-equation based) [36] or variational unitary transformations [37].

In what follows we consider besides the magneto-elastic interaction, Eq. (3.14), another type of spin-phonon coupling [35, 38],

$$\bar{\mathcal{H}}^{\mathrm{II}}_{\mathrm{s-p}} = g\omega_0 \sum_i (b_i^\dagger + b_i)(\vec{S}_i\vec{S}_{i+1} - \vec{S}_i\vec{S}_{i-1})\,, \tag{3.16}$$

where the AF exchange integral varies linearly with the difference between the phonon amplitudes on neighbouring sites, and perform a Schrieffer-Wolff transformation [39], $\tilde{\bar{\mathcal{H}}} = \exp(\mathcal{S})\bar{\mathcal{H}}\exp(-\mathcal{S})$, with

$$\mathcal{S}^{\mathrm{I}} = g\sum_i (b_i^\dagger - b_i)\vec{S}_i\vec{S}_{i+1} \quad \text{and} \quad \mathcal{S}^{\mathrm{II}} = g\sum_i (b_i^\dagger - b_i)(\vec{S}_i\vec{S}_{i+1} - \vec{S}_i\vec{S}_{i-1})\,, \tag{3.17}$$

respectively. In contrast to electron-phonon systems with Holstein coupling, where the (Lang-Firsov) transformation similar to $\exp(S)$ completely removes the electron-phonon interaction term ($\bar{\mathcal{H}}_{\mathrm{e-p}}$), applying the unitary transformation $\exp(S)$ to $\bar{\mathcal{H}}$ with Eqs. (3.14) and (3.16), we obtain an infinite series of terms, which can not be summed up to a simple expression. To derive an effective spin model we now take the average over the (transformed) phonon vacuum. The resulting spin Hamiltonian $\bar{\mathcal{H}}_{\mathrm{eff,s}} = \langle\tilde{0}_{\mathrm{p}}|\tilde{\bar{\mathcal{H}}}|\tilde{0}_{\mathrm{p}}\rangle$ contains longer than next-nearest-neighbour ranged Heisenberg interactions as well as numerous multi-spin couplings. To a good approximation we can neglect them and obtain (cf. [37])

$$\bar{\mathcal{H}}_{\mathrm{eff,s}}^{\mathrm{I/II}} = \sum_i (\vec{S}_i\vec{S}_{i+1} + \alpha_{\mathrm{eff}}^{\mathrm{I/II}}\vec{S}_i\vec{S}_{i+2}) \tag{3.18}$$

with

$$\alpha_{\mathrm{eff}}^{\mathrm{I}} = \frac{\alpha + g^2(1-2\alpha)/2 + 3g^4\omega_0/16 - 37g^4(1-2\alpha)/96}{1 + g^2\omega_0/2 - g^2(1-\alpha)/2 - 3g^4\omega_0/8 + g^4(28-37\alpha)/96}\,, \tag{3.19}$$

$$\alpha_{\mathrm{eff}}^{\mathrm{II}} = \frac{\alpha + g^2\omega_0/2 + g^2(3-5\alpha)/2 + 3g^4\omega_0/48 - g^4(75-124\alpha)/24}{1 + g^2\omega_0 - 3g^2(1-\alpha)/2 - 9g^4\omega_0/8 + g^4(59-75\alpha)/24}\,. \tag{3.20}$$

That is the integration over the phonon subsystem yields an additional frustrating next-nearest-neighbour exchange interaction. Therefore, without any explicit frustration $\alpha$, the effective frustration $\alpha_{\mathrm{eff}}$ due to the phonons can lead to a gap in the energy spectrum and to spontaneous dimerization. This effect is most important in the anti-adiabatic frequency range [37].

In order to determine the critical line in the the $\alpha - g$ plane indicating the transition from the gapless to the gapped ground state, we use the level crossing criterion [25, 23, 37, 38] for the lowest singlet and triplet excitations which become degenerate at $\alpha_c(N)$. At $\alpha_c$ the finite-size corrections $\alpha_c(N) - \alpha_c(\infty) \sim N^{-2}$ are small. The resulting phase diagrams are displayed in Fig. 4. We find that the phase boundary of the original quantum spin-phonon and effective spin models agree surprisingly well, where for the effective model (3.18) $\alpha_c(g)$ can be obtained with high accuracy on local workstations if $N \leq 20$. For spin-phonon coupling of type I the critical curve exhibits a remarkable upturn before crossing the abscissa; i.e., the frustration is suppressed for small spin-phonon coupling, but over-critical for strong coupling. It is this feature which makes it necessary to expand $\tilde{\bar{\mathcal{H}}}$ up to fourth order in $g$ to approximate $\bar{\mathcal{H}}$ in a correct

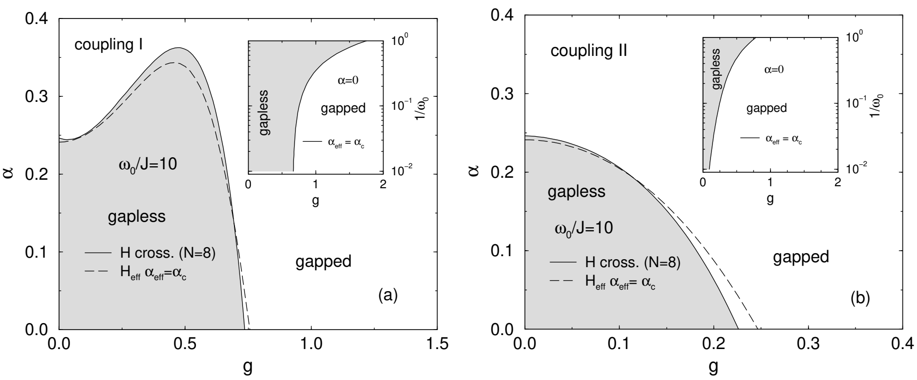


**Figure 4** Phase diagram of the original spin-phonon model (3.13) and the effective spin model (3.18) with spin-phonon couplings of types I (a) and II (b).

way. A second order theory is not capable to describe the observed critical line. The upturn of $\alpha_c(g)$ at small $g$ was reproduced quite recently by linked series expansion techniques [40]. By contrast $\alpha_c(g)$ is a monotonous decreasing function of $g$ for the coupling of type II. It appears that one would get the same shape also for a second order theory. However, to enlarge the application area of our approximation taking into account higher order contributions is still appropriate. For $\alpha \equiv 0$, differently from the coupling case I, $g_c$ tends to zero in the anti-adiabatic limit $\omega_0 \to \infty$. While the $q = 0$ and the $q = \pi$ phonon mode compete in the case of coupling I, allowing for a stable gapless phase up to a critical $g$, there is no interaction with the $q = 0$ mode in $H_{\mathrm{sp}}^{\mathrm{II}}$. Therefore the $q = \pi$ mode induces long ranged exchange more efficiently, leading to a vanishing $g_c$ for $\omega_0 \to \infty$.

### 3.3 RPA approach at T $\neq$ 0: Soft-mode vs. central-peak behaviour

The absence of a soft phonon mode at the displacive SP in $CuGeO_3$ has been puzzling for a long time, since the behaviour was believed to be inconsistent with the standard Cross-Fisher RPA approach to SP transitions [41]. Even worse, the relevant phonon modes harden by about 5% with decreasing temperature [42], pointing to a central peak scenario. A way to reconcile these results within the framework of the Cross-Fisher theory has been proposed by Gros and Werner [43], with the result that a complete phonon softening occurs only for bare phonon frequencies less than a critical value ($\omega_0 < \omega_{0,c} = 2.2T_c$, where $T_c$ is the SP transition temperature. For higher $\omega_0$ a central peak develops reaching $T_c$ from above. For the magnetostrictive Heisenberg spin chain model, however, it was not possible to analyze the complete pole structure of phonon spectral function.

To test this scenario we restrict ourselves to the simpler XY model

$$\bar{\mathcal{H}}_{\rm s}^{\rm XY}=\sum_i(S_i^xS_{i+1}^x+S_i^yS_{i+1}^y)\,,\quad \bar{\mathcal{H}}_{\rm p}=\sum_i\frac{p_i^2}{2M}+\frac{K}{2}(u_i-u_{i+1})^2 \qquad (3.21)$$

with the spin-phonon coupling term

$$\bar{\mathcal{H}}_{\rm s-p}=\frac{\lambda}{2}\sum_i(u_i-u_{i+1})(S_i^+S_{i+1}^-+S_i^-S_{i+1}^+)\,. \qquad (3.22)$$

The above magnetostrictive XY model has been proposed as the minimal model to describe the SP transition [44]. Performing a Jordan-Wigner transformation [45] it can be mapped onto a model of spinless fermions only interacting with the phonon system $\bar{\mathcal{H}}_{\rm p}=\sum_q\omega_q b_q^\dagger b_q$:

$$\bar{\mathcal{H}}_{\rm s}^{\rm XY} \;\to\; \bar{\mathcal{H}}_{\rm e}^{\rm JW}=-\sum_k\cos(k)c_k^\dagger c_k\,, \qquad (3.23)$$

$$\bar{\mathcal{H}}_{\rm s-p} \;\to\; \bar{\mathcal{H}}_{\rm e-p}^{\rm JW}=g\omega_0\sum_{k,q}\eta(k,q)(b_q+b_{-q}^\dagger)c_k^\dagger c_{k-q}\,, \qquad (3.24)$$

where

$$\eta(k,q)=-i\left(\frac{\omega_0}{N\omega_q}\right)^{\frac{1}{2}}[\sin(k-q)-\sin(k)]\,. \qquad (3.25)$$

with $\omega_q=2\omega_0\sin(q/2)$, i.e $\omega_\pi=2\omega_0$.

Determining the equation of motion for the Matsubara phonon Green's function $\bar{D}(q,i\omega_n)$ within the scheme worked out by Bennett and Pytte for the magnetostrictive Heisenberg model [46], the main advantage is that the higher-order spin-spin correlation functions can be calculated without further approximations for the XY-case. The retarded Green's function $\bar{D}^{\rm ret}(q,\omega)$ is obtained from $\bar{D}(q,i\omega_n)$ by analytical continuation $i\omega_n\to\omega$. In the uniform phase above $T_c$, the RPA propagator of the $q=\pi$-phonon, being responsible for the phase transition, then results as

$$\bar{D}^{\rm ret}(\pi,\omega)=\frac{4\omega_0}{\omega^2-4\omega_0^2-2\omega_0\bar{P}(\pi,\omega)}, \qquad (3.26)$$

$$\bar{P}(\pi,\omega)=-(2g\omega_0)^2\int_0^\pi\frac{dk}{\pi}\frac{\sin^2(k)\tanh[\frac{\beta}{2}\cos(k)]}{\omega+2\cos(k)}. \qquad (3.27)$$

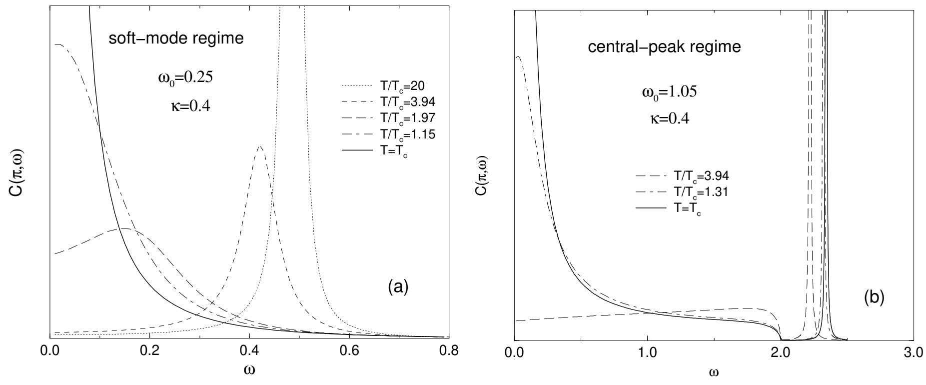


**Figure 5** Dynamical structure factor for the magnetostrictive XY model.

A structural instability occurs if $\bar{D}^{\mathrm{ret}}(q,\omega)$ exhibits a pole at a certain $q$-value for $\omega = 0$. In that case an excitation with arbitrary low energy is possible and the lattice becomes unstable with respect to a (static) deformation with wave number $q$. From this condition the equation for the inverse transition temperature $\beta_c = 1/T_c$ easily follows as

$$1 = \kappa \int_0^{\pi} dk \frac{\sin^2(k) \tanh[\frac{\beta_c}{2}\cos(k)]}{\cos(k)}\,, \tag{3.28}$$

where $\kappa = g^2\omega_0/\pi$. A more detailed study of the complete pole structure of $\bar{D}^{\mathrm{ret}}(q,\omega)$ in both the undimerized and dimerized phases is presented in Ref. [47], where also the ultrasound properties of the system were discussed. Here we focus on the temperature dependence of the dynamical structure factor above $T_c$,

$$C(q,\omega) = -\frac{1}{\pi} \lim_{\delta\to 0} \frac{\mathrm{Im}\ \bar{\mathrm{D}}^{\mathrm{ret}}(\mathrm{q},\omega+\mathrm{i}\delta)}{1-e^{-\beta\omega}}\,, \tag{3.29}$$

which is displayed in Fig. 5 for two characteristic phonon frequencies $\omega_0 = 0.25$ and $\omega_0 = 1.05$, corresponding to the soft-mode (a) and central-peak (b) regimes, respectively. For small bare phonon frequencies the maximum in $C(\pi,\omega)$ is located around $\omega = \omega_\pi$ at high temperatures and moves with decreasing temperatures to lower frequencies until a real divergence of $C(\pi,\omega)$ appears for $T = T_c$ at $\omega = 0$. For large bare phonon frequencies a completely different behaviour is found. Now the high-temperature phonon peak stays around $\omega = \omega_\pi$ and even hardens in some degree as $T \to T_c$. At the same time a peak structure evolves at $q = 0$ which becomes divergent at $T = T_c$. This so-called central peak corresponds to a new collective magneto-elastic excitation of the coupled spin-phonon system, which occurs at the SP transition and moves to higher energies as the temperature is lowered further [47].

## 4 Conclusions

In this report the lattice dynamical effects on the Peierls transition in coupled electron/spin-phonon systems were discussed. Our approach was based on several generic model Hamiltonians obtained from the one-dimensional Holstein/SSH Hubbard model in important limiting cases. Applying both basically exact numerical and approximative analytical methods we are able to calculate both ground-state and spectral properties of these simplified models for the complete range of model parameters. The focus, however, was on non-adiabatic effects due to the phonon dynamics. The presented results confirm previous findings that quantum phonon fluctuations destroy the Peierls distorted state at sufficiently weak electron/spin-phonon interactions.

For the spinless fermion model this means that for weak electron-phonon couplings the system resides in a metallic (gapless) phase described by two non-universal Luttinger liquid parameters. The renormalized charge velocity and the correlation exponent are obtained from finite-size scaling relations, fulfilled with great accuracy. The Luttinger liquid phase splits in an attractive and repulsive regime at low and high phonon frequencies, respectively. Here the polaronic metal, realized for repulsive interactions, is characterized by a strongly reduced mobility of the charge carriers. Increasing the electron-phonon coupling, the crossover between Luttinger liquid and charge-density-wave behaviour is found in excellent agreement with very recent DMRG results. The transition to the CDW state is accompanied by significant changes in the optical response of the system. Most notably seems to be the substantial spectral weight transfer from the Drude to the regular (incoherent) part of the optical conductivity, indicating the increasing importance of inelastic scattering processes in the CDW (Peierls distorted) regime.

As a simple model for a spin-Peierls system we considered a (frustrated) Heisenberg spin chain model supplemented by a coupling to optical phonons with frequencies comparable to the magnetic exchange coupling, which is, e.g.. the relevant limit for the spin-Peierls compound $CuGeO_3$. The magnetic excitations inherently include a local lattice distortion requiring a multi-phonon-mode treatment of the lattice degrees of freedom. When compared to the static model of an alternating, dimerized spin chain the magnetic properties are strongly renormalized due to the coupled spin and lattice dynamics. For the quantum spin-phonon model the dimerization dependence of the spin triplet excitation gap is found to be in qualitative agreement with experiment. In the anti-adiabatic phonon frequency range we used the concept of unitary transformations in order to integrate out phonon degrees of freedom, where the spin-phonon interaction results in an additional frustration in the effective spin-only model. For two types of spin-phonon couplings, the critical lines separating gapless from gapped ground states are found to agree for the original spin-phonon and effective spin models. Finally the reliability of the RPA approach to SP transitions was assessed in terms of an XY model with additional magneto-elastic interaction. With increasing phonon frequency the dynamical displacement structure factor shows a crossover from a soft-mode to central-peak behaviour, normally linked to displacive and order-disorder types of transition respectively. The central peak predicted to appear at $T_c$ for large bare phonon frequency corresponds not to a real phononic but rather to a new magneto-elastic excitation.

## Acknowledgements

The authors would like to thank B. Büchner, H. Büttner, R. J. Bursill, A. P. Kampf, A. W. Sandvik, J. Schliemann, G. S. Uhrig, G. Wellein and R. Werner for valuable discussions. The ED calculations were performed at the LRZ München, NIC Jülich, and HLR Stuttgart.

## Bibliography

[1] R. Peierls, *Quantum theory of solids.*, (Oxford University Press, Oxford 1955).

[2] N. Tsuda, K. Nasu, A. Yanese, K. Siratori, *Electronic Conduction in Oxides.* (Springer-Verlag, Berlin 1990); J.-P. Farges (Ed.), *Organic Conductors.* (Marcel Dekker, New York 1994).

[3] W. P. Su, J. R. Schrieffer, A. J. Heeger, Phys. Rev. Lett. **42**, 1698 (1979).

[4] T. Holstein, Ann. Phys. **8**, 325 (1959); **8**, 343 (1959).

[5] D. Khomskii, W. Geertsma, and M. Mostovoy, Czech. J. Phys. **46**, 3239 (1996).

[6] J. W. Bray, L. V. Interrante, I. S. Jacobs, J. C. Bonner, p. 353 in *Extended Linear Chain Compounds*, ed. J. S. Miller (Plenum, New York 1985).

[7] R. H. McKenzie, J. W. Wilkins, Phys. Rev. Lett. **69**, 1085 (1992).

[8] G. Hutiray, J. Sólyom (Eds.), *Charge Density Waves in Solids*, volume 217 of *Lecture Notes in Physics*, (Springer, Berlin 1985).

[9] L. Degiorgi et al., Phys. Rev. B **52**, 5603 (1995).

[10] M. Hase, I. Terasaki, K. Uchinokura, Phys. Rev. Lett. **70**, 3651 (1993).

[11] M. Braden et al., Phys. Rev. B **54**, 1105 (1996); Phys. Rev. Lett. **80**, 3634 (1998).

[12] R. Werner, C. Gros, M. Braden, Phys. Rev. B **59**, 14356 (1999).

[13] J. E. Lorenzo et al., Phys. Rev. B **50**, 1278 (1994).

[14] J. E. Hirsch, E. Fradkin, Phys. Rev. B **27**, 4302 (1983).

[15] R. J. Bursill, R. H. McKenzie, C. J. Hamer, Phys. Rev. Lett. **80**, 5607 (1998).

[16] R. H. McKenzie, C. J. Hamer, D. W. Murray, Phys. Rev. B **53**, 9676 (1996).

[17] A. Weiße, H. Fehske, G. Wellein, A. R. Bishop cond-mat/0003125.

[18] C. N. Yang, C. P. Yang, Phys. Rev. **150**, 321 (1966); Phys. Rev. **151**, 258 (1966).

[19] F. D. M. Haldane, Phys. Rev. Lett. **45**, 1358 (1980).

[20] B. Bäuml, G. Wellein, H. Fehske, Phys. Rev. B **58**, 3663 (1998).

[21] A. Weiße, H. Fehske, Phys. Rev. B **58**, 13526 (1998).

[22] G. Wellein, H. Fehske, Phys. Rev. B **58**, 6208 (1998).

[23] G. Castilla, S. Chakravarty, V. J. Emery, Phys. Rev. Lett. **75**, 1823 (1995).

[24] F.D.M. Haldane, Phys. Rev. B **25**, 4925 (1982).

[25] K. Okamoto, K. Nomura, Phys. Lett. A**169**, 433 (1993).

[26] R. Chitra, S. Pati, H. R. Krishnamurthy, D. Sen, S. Ramasesha, Phys. Rev. B **52**, 6581 (1995).

[27] S.R. White, I. Affleck, Phys. Rev. B **54**, 9862 (1996).

[28] A. M. Tsvelik, Phys. Rev. B **45**, 486 (1992).

[29] H. Yokoyama, Y. Saiga, J. Phys. Soc. Japan **66**, 3617 (1997).

[30] K. Fabricius et al., Phys. Rev. B **57**, 1102 (1997).

[31] B. Büchner, H. Fehske, A. P. Kampf, G. Wellein, Physica B **259-261**, 956 (1999).

[32] G. Wellein, H. Fehske, A. P. Kampf, Phys. Rev. Lett. **81** 3956 (1998).

[33] D. Augier, D. Poilblanc, E. Sørensen, I. Affleck, Phys. Rev. B **58**, 9110 (1998).

[34] A. W. Sandvik, D. K. Campell, Phys. Rev. Lett. **83**, 195 (1999).

[35] K. Kuboki, H. Fukuyama, J. Phys. Soc. Jap. **56**, 3126 (1987).

[36] G.S. Uhrig, Phys. Rev. B **57**, R14004 (1998).

[37] A. Weiße, G. Wellein, H. Fehske, Phys. Rev. B **60**, 6566 (1999).

[38] R. J. Bursill, R. H. McKenzie, C. J. Hamer, Phys. Rev. Lett. **83**, 408 (1999).

[39] J.R. Schrieffer, P.A. Wolff, Phys. Rev. **149**, 491 (1966).

[40] S. Trebst, N. Elstner, H. Monien, cond-mat/9907266.

[41] M. C. Cross, D. S. Fisher, Phys. Rev. B **19**, 402 (1979).

[42] M. Braden, B. Hennion, W. Reichardt, D. Dhalenne, A. Revcolevschi, Phys. Rev. Lett. **80**, 3634 (1998).

[43] C. Gros, R. Werner, Phys. Rev. B **58**, R14667 (1998).

[44] L. G. Caron, S. Moukouri, Phys. Rev. Lett. **76**, 4050 (1996).

[45] P. Jordan, E. Wigner, Z. Phys. **47**, 631 (1928).

[46] H. S. Bennett, E. Pytte, Phys. Rev. **155**, 553 (1967).

[47] M. Holicki, Diploma thesis, Universität Bayreuth (2000).